RAPID COMMUNICATIONS

PHYSICAL REVIEW B VOLUME 48, NUMBER 23 15 DECEMBER 1993-I

# Complex spatiotemporal dynamics of current filaments in crossed electric and magnetic fields

G. Hüpper,* K. Pyragas,† and E. Schöll
*Institut für Theoretische Physik, Technische Universität Berlin, Hardenbergstrasse 36, D-10623 Berlin, Germany*
(Received 8 April 1993)

We propose a novel model for the nonlinear dynamics of spatiotemporal patterns in semiconductors with negative differential conductivity under the influence of a transverse magnetic field. Dielectric relaxation of both the applied electric field and the Hall field combined with the generation-recombination kinetics of the carriers obtained from a Monte Carlo simulation induces a transverse motion of the current filaments and complex sequences of nucleation, traveling, and destruction of filaments which result in chaotic current and voltage oscillations.

Nonlinear and chaotic spatiotemporal dynamics of electrical transport in semiconductors has attracted considerable theoretical[1] and experimental[2] research to date. In particular, high-purity semiconductors under the simultaneous application of parallel or crossed electric and magnetic fields have been found to exhibit self-generated chaotic current or voltage oscillations under dc bias.[3–9] In the regime of impurity impact ionization breakdown at low temperatures,[4–9] but also in other semiconductor structures and in plasma physics,[10] such oscillatory instabilities are often connected with S-shaped current density-field characteristics and negative differential conductivity (SNDC), which gives rise to current filamentation. For perpendicular electric and magnetic fields, the occurring filaments show either asymmetric breathing states,[9] or travel transversally in the direction of the Lorentz force across the sample.[7] While for positive differential conductivity a mechanism for spatially homogeneous magnetic-field-induced oscillations in terms of a dynamic Hall effect was proposed recently,[11,12] an extension of this model to filamentary conduction is necessary in order to understand these complex spatiotemporal instabilities. This is the purpose of this paper. Up to now, to the best of our knowledge, an adequate theory of filamentary transport in crossed magnetic and electric fields does not exist. Previous qualitative and phenomenological descriptions discussed the dynamics of a single carrier under the influence of the Lorentz force,[7] resulting in a transverse current, or used simple approximations of ordinary differential equations disregarding the space charge in the filament walls.[13]

In this paper we propose a novel physically founded model, which is based upon semiclassical semiconductor transport theory combined with Monte Carlo simulations of the generation-recombination processes, and is able to account for the spatiotemporal degrees of freedom of unipolar nonlinear filamentary conduction and instabilities in crossed electric and magnetic fields. It extends previous work on current filaments[14] which was confined to the case without magnetic field. Following Ref. 11, we neglect quantum effects leading to the splitting of the conduction band into discrete Landau levels of spacing $\Delta E=\hbar\omega_c$, where $\omega_c=e\mathcal{B}/m^*$ with magnetic induction $\mathcal{B}$, elementary charge $e>0$, and effective mass $m^*$. In the impurity breakdown regime the mean energy $E$ per carrier is comparable to the ionization energy $E_{\rm th}$ of the impurities. A classical treatment will thus be applicable in the magnetic-field regime where $\Delta E \ll E_{\rm th}$ holds.[15]

The conduction current density can generally be calculated from the first moment of the Boltzmann equation.[12,16] However, in the regime we are interested in, a constant momentum relaxation time $\tau_m$ may be assumed. In the presence of a magnetic field the current density $\mathbf{j}=qn\mathbf{v}$ is then given by[11,16]

$$\mathbf{j}=en\mu_{\mathcal{B}}\mathbf{F}/q-qn\mu\mu_{\mathcal{B}}(\mathcal{B}\times\mathbf{F}/q)+n\mu^2\mu_{\mathcal{B}}\mathcal{B}(\mathcal{B}\cdot\mathbf{F})\ , \qquad (1)$$

where $n$ is the carrier density, $\mathbf{v}$ is the mean group velocity of the carriers, $q=\pm e$ is their charge, $\mu=\tau_m e/m^*$ is the mobility for $\mathcal{B}=0$, $\mu_{\mathcal{B}}=\mu/(1+\mu^2\mathcal{B}^2)$, $\mathbf{F}=q\mathcal{E}-eDn^{-1}\mu_{\mathcal{B}}^{-1}\nabla_{\mathbf{r}}n$, and $D$ is the diffusion constant.

As the relevant dynamic variables we choose, besides $\mathcal{E}$ and $n$, the densities of carriers bound at $M$ shallow impurity levels $n_i$ $(i=1,\ldots,M)$ corresponding to ground and excited states of donors or acceptors. Transitions between these levels and the band states are possible due to generation-recombination (GR) processes including impact ionization. It is important that both the applied drift field $\mathcal{E}_x$ and the induced Hall field $\mathcal{E}_z$ are treated dynamically reflecting their finite dielectric relaxation time,[11] while $\mathcal{B}$ (applied in $y$ direction) is treated as a control parameter. As the dominant spatial inhomogeneity in the SNDC regime occurs perpendicular to the drift field in the form of current filaments,[1,2] we assume spatial inhomogeneity only in the $z$ direction. The dynamic equations for a sufficiently long sample with ideal planar contacts connected in series with a voltage source $U_0$ and a load resistor $R$ and in parallel with a capacitance $C$ are the continuity equations

$$\frac{\partial n}{\partial t}+\frac{\partial(nv_z)}{\partial z}=\phi(n,\underline{n}_t,\mathcal{E}),\quad \frac{\partial \underline{n}_t}{\partial t}=\underline{\phi}_t(n,\underline{n}_t,\mathcal{E})\ , \qquad (2)$$

and the dielectric relaxation equations

$$c_r\frac{\partial\mathcal{E}_x}{\partial t}=j_0-(\mu_{\mathcal{B}}\langle n\rangle+\sigma_l)\mathcal{E}_x-\mu_{\mathcal{B}}\mu\mathcal{B}\left[\frac{\Delta n}{W}-\langle n\mathcal{E}_z\rangle\right]\ , \qquad (3)$$

$$\partial\mathcal{E}_z/\partial t=-nv_z\ , \qquad (4)$$

supplemented by Maxwell's equations

 

$$\partial \mathcal{E}_x/\partial z=0, \quad \partial \mathcal{E}_z/\partial z=\rho \equiv n+\sum_i^M n_i-1 , \tag{5}$$

where $c_r=1+LC/(\varepsilon A)$, $A=bWL_D^2$ is the lateral cross section of the sample, $L$ is the length in the $x$ direction, $\varepsilon$ is the permittivity, $j_0=U_0/(RAe\mu_l N_A^* \mathcal{E}_0)$, $\sigma_l=\tau_M L L_D/(RA\varepsilon)$, $v_z=\mu_{\mathcal{B}}[\mathcal{E}_z-(1/n)\partial n/\partial z+\mu\mathcal{B}\mathcal{E}_x]$ is the mean velocity in the $z$ direction, $\rho$ is the local charge density, $\phi, \underline{\phi}_t$ are the GR rates [we have introduced $M$-dimensional vector fields $\underline{n}_t=(n_1,\ldots,n_M)$ and $\underline{\phi}_t=(\phi_1,\ldots,\phi_M)$]. The angular brackets denote the spatial mean value $\int_0^W dz/W$, where $W$ is the width of the sample, and $\Delta n \equiv n(W)-n(0)$. Note that these equations hold for holes ($q=e$), but can easily be adapted to electrons by inverting the sign of $\mathcal{E}_z$. All quantities are given in dimensionless units, i.e., $\mu$, $t$, $z$, $\mathcal{E}$, and $n, \underline{n}_t$ are scaled by the low-field mobility $\mu_l$, the dielectric relaxation time $\tau_M=\varepsilon/(e\mu_l N_A^*)$, the Debye length $L_D=[k_B T_L \varepsilon/(e^2 N_A^*)]^{1/2}$, the thermal field $\mathcal{E}_0=k_B T_L/(eL_D)$, and the effective acceptor concentration $N_A^*=N_A-N_D$, respectively. The classical static Hall effect is reproduced by the homogeneous steady states (denoted by an asterisk): $\mathcal{E}_z^*=-\mu\mathcal{B}\mathcal{E}_x^*$, $j_0=n^*\mu\mathcal{E}_x^*$. We now consider the case that the static $j_0(\mathcal{E}_x^*)$ characteristic exhibits SNDC.[1] The stability of the homogeneous stationary states $\Phi^*=(n^*, \underline{n}_t^*, \mathcal{E}_x^*, \mathcal{E}_z^*)$ with respect to fluctuations $\delta\Phi(z,t)\propto e^{ikz}e^{\lambda t}$ can be investigated by linearization of (2)–(5). Due to (5) only homogeneous modes ($k=0$) allow for $\delta\mathcal{E}_x\neq 0$. This motivates a separate treatment for homogeneous and inhomogeneous modes.

The homogeneous modes yield oscillatory instabilities previously found for the dynamic Hall effect.[11,12] For the inhomogeneous case we obtain a new spatiotemporal instability. From (2)–(5) the eigenvalue equation

$$(\lambda+\mu_{\mathcal{B}} n^*)\frac{H(\lambda)}{G(\lambda)}=\mu_{\mathcal{B}}\left[-k^2+ik(\mu\mu_{\mathcal{B}})^{1/2}\mathcal{B}\frac{F(\lambda)}{G(\lambda)}\right] \tag{6}$$

can be derived, where $G(\lambda)=\det(B-\lambda)$, $B_{ij}=\partial\phi_i/\partial n_j$, $H(\lambda)=G(\lambda)-\sum_{i,j}\mathrm{adj}(B-\lambda)_{i,j}d_j=\det(A_{\mathrm{GR}}-\lambda)$, $d_i=\partial\phi_i/\partial n$, and $(\mathrm{adj}B)_{i,j}$ is $(-1)^{i+j}$ times the determinant of the matrix obtained by deleting the $j$th row and the $i$th column of $B$ (adjunct of $B$). $A_{\mathrm{GR}_{i,j}}$ is $B_{i,j}-d_j\delta_{i,j}$ and describes charge-neutral fluctuations with $\delta\mathcal{E}_z=0$, $\delta\rho=0$, and $F(\lambda)=-\sum_{i,j}\mathrm{adj}(B-\lambda)_{i,j}e_j$ with $e_i=\partial\phi_i/\partial\mathcal{E}$ and $\mathcal{E}=(\mathcal{E}_x^2+\mathcal{E}_z^2)^{1/2}$.

Bifurcations with $\lambda(k=0)=0$ are possible at the turning points of an SNDC regime of the current density-field characteristic.[1] At these points we expand (6) for small $k,\lambda$, restricting our analysis to the case of two impurity levels ($M=2$): $\lambda(k)=ivk-\tilde{D}k^2$ and get

$$v=(\mu\mu_{\mathcal{B}})^{1/2}\mathcal{B}(\partial\rho/\partial\mathcal{E})[(\partial\phi_1/\partial n_1)(\partial\phi_2/\partial n_2)-(\partial\phi_2/\partial n_1)(\partial\phi_1/\partial n_2)]/\{n^*[-(\partial\phi_1/\partial n_1)-(\partial\phi_2/\partial n_2)-(\partial\phi/\partial n)]\} . \tag{7}$$

It can be shown under general conditions that $v$ has the opposite sign of $\mathcal{B}$. Thus the fluctuation moves *transversally in the direction of the Lorentz force.* The velocity is proportional to $\mathcal{B}$ for small $\mathcal{B}$ in agreement with experiment,[7] until $\mu_{\mathcal{B}}$ differs significantly from $\mu$. The effective diffusion coefficient $\tilde{D}=D_0+\mu\mathcal{B}^2 D_{\mathcal{B}}$ can be split in a $\mathcal{B}$-independent part $D_0$ and $\mu\mathcal{B}^2 D_{\mathcal{B}}$ with

$$D_0=\frac{(\partial\phi_1/\partial n_1)(\partial\phi_2/\partial n_2)-(\partial\phi_2/\partial n_1)(\partial\phi_1/\partial n_2)}{-n^*[(\partial\phi_1/\partial n_1)+(\partial\phi_2/\partial n_2)+(\partial\phi/\partial n)]}>0 , \tag{8}$$

$$D_{\mathcal{B}}=\mu_{\mathcal{B}}(F/G)'FG/(n^*H'^2)-F^2/(n^{*3}H'^2) -\mu_{\mathcal{B}}[F^2/(2n^{*2}H'^3)][(H''G-2G'H')/G^2] , \tag{9}$$

where the prime denotes the derivative with respect to $\lambda$, and the argument $\lambda=0$ is taken.

To get a physical idea of this remarkable transverse motion of the fluctuations, we consider a carrier density fluctuation around the unstable homogeneous state with and without a magnetic field. This fluctuation will grow in both cases due to the GR instability. Thus a fluctuation of the transverse electric field will be built up according to (4), so that the drift and diffusion currents will tend to cancel each other: $n\delta\mathcal{E}_z=\partial\delta n/\partial z$. In the case $\mathcal{B}=0$ this will lead to a *symmetric* change of the absolute value of the electric field, since $\mathcal{E}_z^*=0$. This local increase of the electric field results in a symmetric increase of the fluctuation due to the GR processes. In the case $\mathcal{B}\neq 0$ the fluctuation $\delta\mathcal{E}_z$ will *reduce* the absolute value of the electric field on one side, while it will *increase* it on the opposite site. Due to the GR processes the side of the fluctuation with lower electric field will decrease and the opposite side will increase. As a result, the fluctuation will move in the direction of the Lorentz force. Note that in this picture only the shape of the fluctuation moves transversally while the carriers themselves remain at their transverse positions, performing free to bound transitions and vice versa. This corrects the former view of traveling filaments being due to individual carriers moving in the direction of the Lorentz force.[7] Rather, the situation is analogous to the motion of water molecules in a water wave.

We have simulated the system numerically for $p$-type Ge at 4 K with $c_r=1$, $\sigma_l=0$ (current control) in the impurity breakdown regime with GR rates $\phi=X_1^s n_2-T_1^s n(1+c-n_1-n_2)+X_1 n n_1+X_1^* n n_2$, $\phi_1=T^* n_2-X^* n_1-X_1 n n_1$, $\phi_2=-\phi-\phi_1$, where $c=N_D/N_A^*$ is the compensation. The GR coefficients have been obtained for a two-impurity-level model[1] (ground and excited level) from a spatially homogeneous Monte Carlo simulation with $\mathcal{B}=0$ (Ref. 14) and scaling the electric field $\mathcal{E}$ by a factor $(1+\mu^2\mathcal{B}^2)^{-1/2}$. This is possible because we have assumed constant mobility. The resulting $j_0(\mathcal{E}_x^*)$ characteristic shows SNDC (Fig. 1). The Monte Carlo data have been fitted by smooth functions (see Fig. 1) and substituted into the differential equations (2)–(5) which have been solved with the aid of the method of particles[17,18] using cyclic transverse boundary conditions. Our nonlinear spatiotemporal analysis predicts the formation of current filaments on

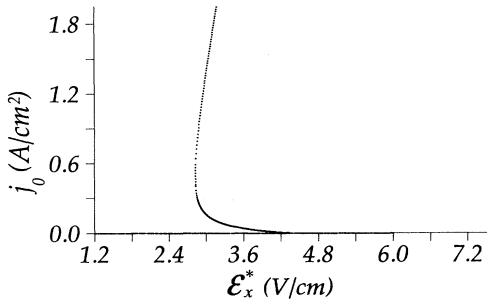


FIG. 1. Static current density-field characteristic calculated with $N_A=10^{14}$ cm$^{-3}$, $N_D=5\times10^{12}$ cm$^{-3}$, $\varepsilon=16\varepsilon_0$, $T_L=4$ K, $\mu=\mu_l=10^5$ cm$^2$/V s, $\tau_M=10^{-12}$ s, $L_D=5.6\times10^{-6}$ cm, $\mathcal{E}_0=60.8$ V/cm, $X^*=10^{-15}$, $T^*=7.21\times10^{-5}$, $X_1^s=1.4\times10^{-6}$, $\alpha=60.8(1+\mu^2\mathcal{B}^2)^{-1/2}$, $X_1(\mathcal{E})=7.85\times10^{-4}\times\exp[-11.3(\alpha\mathcal{E})^{-0.745}]$, $X_1^*(\mathcal{E})=4.18\times10^{-2}\times\exp[-3.72(\alpha\mathcal{E})^{-0.66}]$, $T_1^s(\mathcal{E})=-1.2\times10^{-3}\times\exp[-0.2(-0.254+\alpha\mathcal{E})^2]+1.73\times10^{-3}(0.421+\alpha\mathcal{E})^{-0.887}$.

the NDC branch of the current density-field characteristic. These filaments move in the direction of the Lorentz force (Fig. 2). After some transients the filament travels with a constant velocity $v$. Figure 3 shows $v$ as a function of the applied magnetic field. Additionally, the velocity obtained by the linear stability analysis (6) is plotted. The latter is larger because it describes only *small* fluctuations from the *NDC state*. Note that the velocity ($\approx10^2-10^3$ cm/s) is much smaller than the drift velocity of the carriers ($\approx10^5-10^6$ cm/s), in agreement with experiment.[7]

For a finite sample with Dirichlet boundary conditions[14] $\mathcal{E}_z(0,t)=\mathcal{E}_z(W,t)=0$ the filament travels to the boundary and is pinned there. This behavior changes if other contact geometries are used. We demonstrate this for triangular contacts (Fig. 4) which may also serve as a model for *nonideal* planar Ohmic contacts.[7] In this case the length of the sample $L=L_0+2L'|z-W/2|/W$ is a function of the transverse coordinate. Due to our assumption of homogeneity in the $x$ direction we restrict ourselves to small contact angles, i.e., $L'/W$ should be small against logarithmic derivatives like $(\partial \ln n/\partial z)$. In this case the model equations read

$$\partial(Ln)/\partial t+\partial(Lnv_z)/\partial z=L\phi\ , \tag{10}$$

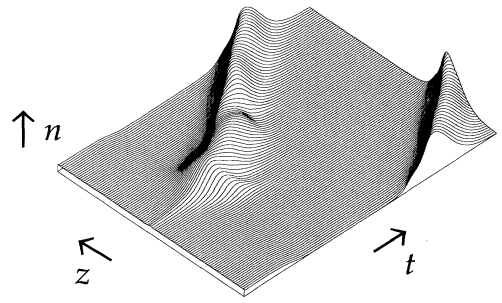


FIG. 2. Spatiotemporal dynamics of the carrier density $n(z,t)$ in the presence of an externally applied magnetic field under cyclic boundary conditions for $j_0=34$ mA/cm$^2$, $\mathcal{B}=10$ mT with planar contacts. The total time is $8.1\times10^{-6}$ s, the sample width is $W=90$ $\mu$m.

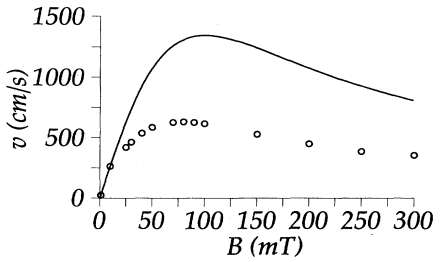


FIG. 3. Transverse velocity of the traveling filaments as a function of the magnetic field for $j_0=93.76$ mA/cm$^2$, $W=120$ $\mu$m from the nonlinear simulation (dots). The full line shows the velocity obtained by the linear stability analysis for the same control parameters.

$$\gamma\frac{\partial U}{\partial t}=j_0-(\mu_{\mathcal{B}}\langle n/L\rangle+\sigma_l')U-\mu_{\mathcal{B}}\mu\mathcal{B}\left[\frac{\Delta n}{W}-\langle n\mathcal{E}_z\rangle\right], \tag{11}$$

$$\partial(L\mathcal{E}_z)/\partial z=L\rho,\quad L\mathcal{E}_x=\text{const}\equiv U(t) \tag{12}$$

with $\gamma=\langle 1/L\rangle+C/(\varepsilon A)$, $\sigma_l'=\tau_M/(RA\varepsilon)$.

Qualitatively, these contacts yield the following scenario: the free carriers inside the moving filament will be spread over an increasing effective sample length $L(z)$, which reduces the maximum carrier density in the filament. Additionally, the drift field and therefore the generation rate decrease. Both effects tend to destroy the filament. As a result, the current through the sample decreases, which increases the voltage of the sample and thus enhances the filament due to increased generation rates.

The time scales of these processes are given by the time the filament needs to travel across the sample, the GR time, and the dielectric relaxation time of the electric field.

Depending upon the ratios of these time scales and the geometry of the contacts, different states of the filament are possible. For small magnetic fields and comparable time scales the filament rests in the middle of the sample

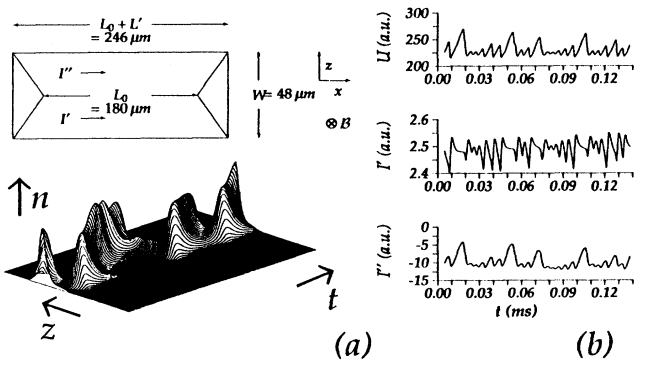


FIG. 4. Traveling filaments for $j_0=0.85$ mA/cm$^2$, $\mathcal{B}=20$ mT with triangular contacts. The inset shows the sample geometry. (a) Spatiotemporal dynamics of $n(z,t)$. The total time is $2\times10^{-5}$ s. (b) Time series of the sample voltage $U(t)$ and currents $I',I''$ (see inset), all in arbitrary units.

and shows an asymmetric breathing of the filament walls as observed in $n$-type GaAs.[19,9]

A more complex dynamic behavior is found if the dielectric relaxation and the destruction of the filament through the GR processes are slower than the transverse motion of the filament. Such a situation is shown in Fig. 4(a). The filament travels in the direction of the Lorentz force. Due to the inertia of the dielectric relaxation the drift field increases slowly. This supports destruction of the filament, so that with increasing voltage a new filament in the middle of the sample can be generated. This successive nucleation, traveling, and destruction of filaments leads to slow chaotic voltage and current oscillations [Fig. 4(b)] and has indeed been found in recent experiments on $p$-type Ge.[7]

As a function of magnetic field, above a minimum threshold $\mathcal{B}$, we find successively asymmetric breathing oscillations; small regular oscillations due to periodic nascence and destruction of traveling filaments; chaotic oscillations due to intermittent nascence and destruction; pinning of the filaments at the transverse boundary after some transient traveling sequences.

In conclusion, we have developed a semiconductor model for filamentary transport in crossed electric and magnetic fields in the regime of SNDC, which predicts a variety of complex self-organized spatiotemporal nonlinear behavior. Using generation-recombination rates obtained from a Monte Carlo simulation with no adjustable parameters, we are able to explain transverse motion of filaments in the direction of the Lorentz force, and chaotic sequences of nucleation, traveling, and destruction of filaments in good agreement with recent experiments in the regime of low-temperature impurity breakdown.

This work was partially supported by Alexander von Humboldt-Stiftung and Deutsche Forschungsgemeinschaft.

---

*Present address: Aescudata GmbH, Bahnhofstr. 37, D-21423 Winsen (Luhe), Germany.

†Permanent address: Institute of Semiconductor Physics, 2600 Vilnius, Lithuania.

[1]E. Schöll, *Nonequilibrium Phase Transitions in Semiconductors* (Springer-Verlag, Berlin, 1987).

[2]J. Peinke, J. Parisi, O. E. Rössler, and R. Stoop, *Encounter with Chaos* (Springer-Verlag, Berlin, 1992).

[3]G. A. Held, C. Jeffries, and E. E. Haller, Phys. Rev. Lett. **52**, 1037 (1984).

[4]X. N. Song, D. G. Seiler, and M. R. Loloee, Appl. Phys. A **48**, 137 (1989).

[5]J. Spinnewyn, H. Strauven, and O. B. Verbeke, Z. Phys. B **75**, 159 (1989).

[6]K. Aoki, Y. Kawase, K. Yamamoto, and N. Mugibayashi, J. Phys. Soc. Jpn. **59**, 20 (1990).

[7]W. Clauss, U. Rau, J. Peinke, J. Parisi, A. Kittel, M. Bayerbach, and R. P. Huebener, J. Appl. Phys. **70**, 232 (1991).

[8]J. Peinke, U. Rau, W. Clauss, R. Richter, and J. Parisi, Europhys. Lett. **9**, 743 (1989).

[9]A. Brandl, W. Kröninger, W. Prettl, and G. Obermair, Phys. Rev. Lett. **64**, 212 (1990).

[10]F.-J. Niedernostheide, B. S. Kerner, and H.-G. Purwins, Phys. Rev. B **46**, 7559 (1992).

[11]G. Hüpper and E. Schöll, Phys. Rev. Lett. **66**, 2463 (1991).

[12]G. Hüpper, E. Schöll, and A. Rein, Mod. Phys. Lett. B **6**, 1001 (1992).

[13]A. Brandl and W. Prettl, Phys. Rev. Lett. **66**, 3044 (1991).

[14]G. Hüpper, K. Pyragas, and E. Schöll, Phys. Rev. B **47**, 15 515 (1993).

[15]A. C. Beer, *Galvanomagnetic Effects in Solids,* Vol. 4 of *Solid State Physics Supplement* (Academic, New York, 1965).

[16]R. A. Smith, *Semiconductors* (Cambridge University Press, Cambridge, 1964).

[17]R. W. Hockney and J. W. Eastwood, *Computer Simulation Using Particles* (McGraw-Hill, New York, 1981).

[18]A. Cenys, G. Lasiene, and K. Pyragas, Solid State Electron. **35**, 975 (1992).

[19]A. Brandl, M. Völcker, and W. Prettl, Appl. Phys. Lett. **55**, 238 (1989).